NANO LETTERS

2008
Vol. 8, No. 8
2517-2525

Improved Biocompatibility and Pharmacokinetics of Silica Nanoparticles by Means of a Lipid Coating: A Multimodality Investigation

Matti M. van Schooneveld,[†] Esad Vucic,[‡] Rolf Koole,[†] Yu Zhou,[‡] Joanne Stocks,[§] David P. Cormode,[‡] Cheuk Y. Tang,[‡] Ronald E. Gordon,[||] Klaas Nicolay,[⊥] Andries Meijerink,[†] Zahi A. Fayad,[‡] and Willem J. M. Mulder*,[‡]

Condensed Matter and Interfaces, University Utrecht, P.O. Box 80000, 3508 TA Utrecht, The Netherlands, Sinai Translational and Molecular Imaging Institute and Imaging Science Laboratories, Mount Sinai School of Medicine, One Gustave L. Levy Place, New York, New York 10029, EM Facility, Department of Pathology, Mount Sinai Hospital, One Gustave L. Levy Place, New York, New York 10029, Cardiovascular Research Center, Mount Sinai School of Medicine, One Gustave L. Levy Place, New York, New York 10029, and Biomedical NMR, Department of Biomedical Engineering, Eindhoven University of Technology, PO Box 513, 5600 MB Eindhoven, The Netherlands

Received June 4, 2008; Revised Manuscript Received June 14, 2008

ABSTRACT

Silica is a promising carrier material for nanoparticle-facilitated drug delivery, gene therapy, and molecular imaging. Understanding of their pharmacokinetics is important to resolve bioapplicability issues. Here we report an extensive study on bare and lipid-coated silica nanoparticles in mice. Results obtained by use of a wide variety of techniques (fluorescence imaging, inductively coupled plasma mass spectrometry, magnetic resonance imaging, confocal laser scanning microscopy, and transmission electron microscopy) showed that the lipid coating, which enables straightforward functionalization and introduction of multiple properties, increases bioapplicability and improves pharmacokinetics.

Monodisperse ensembles of silica nanoparticles can be elegantly synthesized over a wide range of desired sizes using the Stöber synthesis (50−1000 nm)[1] or microemulsion synthesis procedures (≤50 nm).[2] Such monodisperse silica spheres have been investigated extensively as model systems to study fundamental colloidal phenomena, such as interparticle interactions, phase equilibriums, and crystallization.[3] In the past decade, silica-based nanoparticles have increasingly been exploited for numerous biomedical and biotechnological applications. Their utility in these fields ranges from (targeted) drug delivery[4–6] to controlled drug release[7–9] to gene[10–12] and protein[13] delivery or as a carrier vehicle for contrast generating materials. In vitro[14,15] and in vivo[16] fluorescence imaging (FI) as well as in vivo magnetic resonance imaging (MRI)[17,18] have been performed using silica-based nanoparticles. In addition to carrying contrast-generating material for a single imaging modality, the ease of incorporation of different chemicals in silica makes it an excellent material for the integration of multiple properties to enable multimodality biomedical imaging. For example, combined FI and MRI have been shown in vitro[19–23] as well as in vivo.[24,25] Other promising, silica-based materials for combined FI and MRI,[26–29] combined FI and computed tomography (CT),[30] MRI and CT,[31] and even FI, MRI, and CT[32] have been reported but have not yet shown their applicability in vitro or in vivo. Moreover, combined diagnostics and therapeutics (theranostics) using silica nanoparticles has been accomplished[33] and demonstrated to be effective in vitro.[34–36] In addition to the size and composition, the shape and surface properties of silica can be well controlled.

Despite all the aforementioned examples of the utility of silica for biomedical applications, however, a serious draw-

* Corresponding author: e-mail, willem.mulder@mountsinai.org; fax, +1 212 534 2683.

[†] Condensed Matter and Interfaces, University Utrecht.

[‡] Sinai Translational and Molecular Imaging Institute and Imaging Science Laboratories, Mount Sinai School of Medicine.

[§] Cardiovascular Research Center, Mount Sinai School of Medicine.

[||] Department of Pathology, Mount Sinai Hospital.

[⊥] Department of Biomedical Engineering, Eindhoven University of Technology.

10.1021/nl801596a CCC: $40.75
Published on Web 07/12/2008

back of these inorganic nanoparticles is their inherently low biocompatibility as compared to nanoparticles comprised of naturally occurring molecules, such as liposomes or micelles that are composed of phospholipids. Furthermore, silica dispersions are charge-stabilized through Coulomb repulsion between reduced hydroxyl groups $S-O^{23}$ on their surfaces, which poses a limit on their bioapplicability. Especially when administered intravenously, a frequently used route for targeted delivery, rapid silica particle aggregation is observed.[6,37] This aggregation is accelerated through the absorption of opsonins (markers which enhance endocytosis), which is followed by extravascularisation via the reticuloendothelial system (RES).[6,38,39] Consequently, these nanoparticles suffer from poor pharmacokinetics, such as short blood circulation half-life values and accumulation in the lung capillary vessels when administered intravenously.[6,37]

To deal with these limitations, two strategies have been developed aimed at increasing the biocompatibility of silica particles. In the first approach silanols with a short functional group are covalently conjugated to silanol groups on the silica surface, which results in free amine,[40,41] thiol, carboxyl,[42] carboxylate, or phosphonate[5,43] groups on the particle exterior. In the second approach, which is basically a variation of the first approach, the chemical attachment of silanols conjugated with large molecules, that is, block copolymers,[44] poly(ethylene glycol) (PEG),[45–47] or phospholipids,[48] is achieved. Although the silica surface might be neutralized by these techniques, both strategies have serious limitations. For instance, short functional groups are easily subject to opsonization[38] and not always stable against aggregation,[5] while the chemical attachment of bulky molecules is likely to result in low-density surface coatings. Furthermore, neither method can be applied generally to other inorganic nanomaterials and, importantly, once these strategies have been applied to render silica particles bioapplicable, their actual in vivo applicability is seldom investigated.

To address these issues we have recently reported a novel method to obtain hydrophobic silica nanoparticles coated with a physically adsorbed (not covalently attached) monolayer of PEGylated phospholipids. Although physically absorbed lipid bilayers on hydrophilic silica particles have been subject to extensive study,[49,50] lipid monolayers on hydrophobic silica are hardly studied[51] and their ability to render silica particles bioapplicable, and thus to use them as contrast agents or drug delivery systems, is investigated here for the first time. This highly flexible coating method allows, next to the inclusion of PEGylated lipids, the inclusion of many other lipids, for example, paramagnetic lipids for MRI and biofunctional lipids to achieve target specificity. By applying this strategy to quantum dot (QD) containing silica nanoparticles, we were able to create an $\alpha_v\beta_3$-specific nanoparticle that exhibited both fluorescent and paramagnetic properties. This nanoparticle allowed us to image $\alpha_v\beta_3$-integrin expression on cultured endothelial cells in vitro using multiple imaging technologies, that is, fluorescence microscopy, FI, and MRI.[52]

In the current study we investigated the short-term cytotoxicity and pharmacokinetics (blood circulation half-life value and biodistribution) of paramagnetic and PEG-lipid-coated quantum dot containing silica nanoparticles using a wide variety of complementary techniques at different levels, that is, at organ level using MRI, FI, and inductively coupled plasma mass spectrometry (ICP-MS), at tissue and cellular level using confocal scanning laser microscopy (CSLM) and at subcellular or single nanoparticle level using transmission electron microscopy (TEM). The results were compared with those obtained with bare silica nanoparticles (containing QDs but no lipid coating) of the same size.

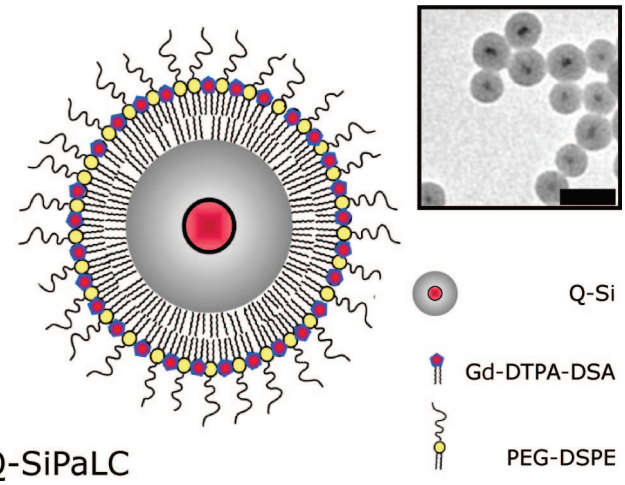

Figure 1. Schematic representation of a Q-SiPaLC (QD containing silica particle with a paramagnetic lipid coating). The inset shows a TEM image (scale bar is 50 nm) of highly monodisperse, QD-containing, and hydrophilic silica particles (Q-Si). Schematic representations of Q-Si, Gd-DTPA-DSA, and PEG-DSPE lipids are shown in the legend.

High-quality single core−shell−shell (CSS) QDs with an average diameter of 7.8 ± 1.0 nm and a quantum efficiency (QE) >55% ($\lambda_{abs} = 606$ nm; $\lambda_{em} = 623$ nm) were synthesized according to the conventional organometallic synthesis route, described in detail elsewhere.[53] The QDs were incorporated in the center of highly monodisperse silica particles with a mean size of 34.3 ± 4.6 nm. These silica particles were made hydrophobic by a condensation reaction of octadecanol (ODOH) on their surfaces. After incorporation, the CSS-QDs retained high quantum efficiency (QE) of 35%.[54] For improved bioapplicability and introduction of paramagnetic properties, the hydrophobic silica particles were subsequently coated with equal amounts of both PEGylated and Gd-DTPA-based lipids[52] (see Supporting Information for synthesis details). A schematic representation of these lipid-coated silica particles or Q-SiPaLCs (QD containing silica particles with a paramagnetic lipid coating) is depicted in Figure 1, together with a TEM image of QD-containing silica particles that were not made hydrophobic and not coated with lipids (inset), to which we will also refer as Q-Si (QD containing silica particles) or bare silica particles throughout the rest of this paper.

Cell viability assays that quantified the amount of surviving cells were subsequently carried out on murine J744A.1 macrophages with different concentrations of lipid-coated or bare silica particles and for varying incubation times ($n = 3$ for each point). The tests relied on a cell-permeant

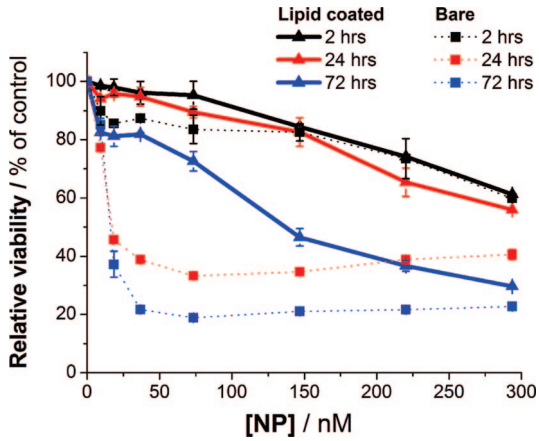

Figure 2. Effects of different concentrations Q-SiPaLCs (triangles & solid line) and Q-Sis (squares and dotted line) on J744A.1 macrophage cell viability after 2 (black), 24 (red), and 72 (blue) h of incubation ($n = 3$). Coating the silica particles with a lipid monolayer increased the number of surviving cells.

reagent which, when coupled to active protease in living cells, generated fluorescence. The signal intensities were quantified with a plate reader. At incubation times of 1 or 3 days with lipid-coated particles, the number of surviving cells was found to be considerably higher as compared to cells incubated with bare silica particles. However no significant difference between lipid-coated or bare particles was observed following 2 h of incubation (Figure 2). Experiments were also repeated with trypan blue (a dye that darkens dead cells) to confirm trends (data not shown). These results indicated that bare silica particles are not acutely toxic but rather cause cell death in the course of days and, importantly, that coating silica particles with a lipid monolayer is an effective way to diminish macrophage cell death. Since macrophages are highly phagocytotic as compared to other cell types, the uptake of the particles is high. Therefore, it may be expected that a better survival rate will be found with nonphagocytotic cell types.

For in vivo studies, 22 C57bl6 mice were included that were injected intravenously with either lipid-coated silica nanoparticles or bare silica nanoparticles via a catheter placed in the tail vein. The animals were housed and maintained at the Mount Sinai Animal Facility. The Mount Sinai School of Medicine Institute of Animal Care and Use Committee approved all experiments.

The blood circulation half-lives of the lipid-coated and bare silica particles were investigated using two different methods. For both methods 14 nmol/kg particles were administered to mice whose hair on their lower limbs had been removed. Blood was drawn sequentially from the saphenous veins before and 5, 20, 60, 120, 240, and 1440 min postinjection of the lipid-coated silica particles. The blood draws for the bare silica particles, which we anticipated to exhibit shorter circulation half-lives, were taken before and 5, 15, 30, 45, 60, 120, and 240 minutes postinjection. Blood (10−20 μL) was collected at each time point and resuspended into preweighed vials containing 80 μL of heparin. The vials were weighed again to determine the volume of blood drawn, taking the density of blood to be 1.05 g/mL.[55] Next, the vials were assessed for cadmium and gadolinium content (the latter only in the case of lipid-coated particles) using ICP-MS ($n = 3$ for each particle), while a parallel set of vials, taken at the same time points, was centrifuged to separate red blood cells from blood plasma. The near-transparent and nonadsorbing blood plasma could be investigated using quantitative fluorescence imaging, since the silica nanoparticles carried highly luminescent QDs in their center. To that end, the samples were placed in the Xenogen IVIS 200, excited for 1 min with light filtered by the GFP background band (410−440 nm), while the photon emission was quantitatively recorded between 610 and 630 nm ($n = 2$ for each particle). In Figure 3 typical fluorescence images of vials containing plasma samples collected from mice injected with lipid-coated (Figure 3A) or bare silica nanoparticles (Figure 3B) are depicted. These pictures show the extended fluorescence activity of lipid-coated particle containing plasma in time, compared to bare particle containing plasma, and thus revealed a considerably longer circulation half-life for lipid-coated silica particles in blood. For both analysis methods, that is, cadmium content or photon count analysis, the values were adjusted for the blood volume. Half-lives were determined by monoexponential fitting of the normalized variance of blood cadmium content or photon count over time (Figure 3C). The half-lives determined with ICP-MS were 14 ± 2 and 162 ± 34 min for the bare and lipid-coated silica nanoparticles, respectively. The values closely resembled the ones determined by fluorescence imaging, being 18 ± 3 min for bare nanoparticles and 165 ± 28 min for lipid-coated nanoparticles. For comparison we note that in one of the very few in vivo studies with intravenously administered silica particles (600 nm diameter particles in Wistar rats), more than 90% blood clearance of the particles was observed within 30 min.[37] Furthermore, the gadolinium content was determined by ICP-MS for the lipid-coated silica particles, and it was found that the molar Gd/Cd ratio in blood had a constant average value of 2.95 ± 0.34 at all time points postinjection of the particles. Importantly, the ratio was identical to that of the original contrast agent before injection. These results indicate that the lipid coating is robust and that the Gd-DTPA-based lipids do not dissociate from the nanoparticles in the vasculature under physiological conditions.

Gd-DTPA-DSA incorporation in the lipid-coated silica particles enabled dynamic MRI of the aorta using a 9.4 T MRI ($n = 3$; Figure 4). The longitudinal ionic relaxivity r_1 of the Gd-DTPA-DSA coated particles was found to be 14.4 mM^{-1} s^{-1}.[52] Taking into consideration that a 35 nm particle carries approximately 6400 lipid molecules, half of which are Gd-DTPA-DSA, the relaxivity per particle was estimated to be 46000 mM^{-1} s^{-1}. Clear enhancement of the vasculature, compared to the prescan, was observed up to at least 2 h postintravenous administration of the contrast agent (45 μmol of Gd/kg), confirming the long-circulation half-life value of the lipid-coated silica particles and demonstrating the effective use of the agent for MRI.

In addition to the circulation half-life, it is important to study the distribution of the silica particles over the different

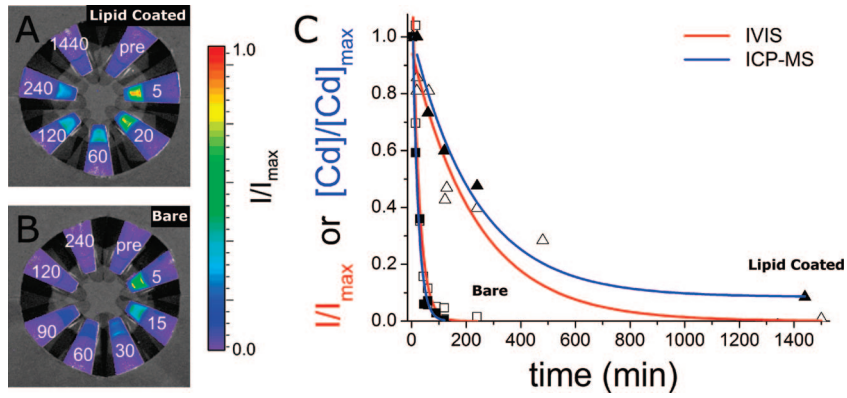

Figure 3. Determination of Q-SiPaLC and Q-Sis blood circulation half-life values. Fluorescence intensity, resulting from the QDs in Q-SiPaLCs (A) and Q-Sis (B), was quantified in blood plasma taken at different time points (indicated in minutes) postinjection ($n = 2$). (C) Alternatively, cadmium determination with ICP-MS was done on blood samples ($n = 3$) and both sets of results were plotted and fitted (blue fit of closed symbols for ICP-MS; red fit of open symbols for FI) to determine the half-life values of Q-SiPaLCs (triangles) and Q-Sis (squares).

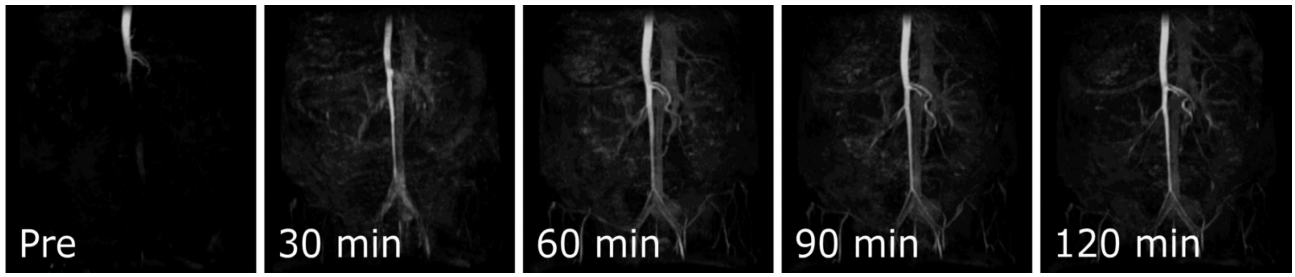

Figure 4. Dynamic MRI of the aorta of mice prior to and at several time points post-Q-SiPaLC administration. The long half-life of the agent resulted in enhancement of the vasculature up to at least 2 h postinjection ($n = 3$).

organs in the mice bodies. This aspect was investigated at the organ (ICP-MS and FI), tissue and cellular (CSLM), and subcellular or single nanoparticle level (TEM).

Liver, spleen, kidney, and heart from control mice and mice sacrificed 1, 4, and 24 h postinjection of the nanoparticles were imaged using the Xenogen IVIS 200. The organs were excited for 40 s with light filtered by the DS Red band (500−550 nm), while the photon emission was recorded using a 610−630 nm filter ($n = 2$ for each time point and particle). Analysis of the data showed that the fluorescence signal in the liver of mice injected with lipid-coated silica particles increased gradually in time, while negligible fluorescence signal was obtained from spleen, heart, and kidneys (Figure 5A). This gradual accumulation (fluorescence intensity from the liver had not reached its maximum value at 4 h postinjection) is in agreement with the long half-life value of the lipid-coated silica particles (∼165 min, see Figure 3). In the case of the bare silica particles the fluorescence signal from the liver increased significantly, while spleen, heart, and kidneys signal were negligible. Contrary to the lipid-coated particles, maximum fluorescence signal in the liver was observed as early as 1 h postinjection. Their massive and rapid accumulation in the liver explains their short circulation half-life (∼15 min, see Figure 3). In time, fluorescence signal from the liver decreased, indicative of a possible particle clearance. Although liver clearance of bare silica particles is not well understood, it has been observed previously for 50 and 250 nm bare silica particles.[6]

Quantitative analysis of the organ distribution of the particles was done by ICP-MS cadmium content determination in organs from control mice and mice sacrificed 1, 4, and 24 h postinjection of the nanoparticles ($n = 1$ for each point and particle, Figure 6). Cadmium determinations allowed for comparison between the lipid-coated and bare silica particles since both types of particle contain equal amounts of this element, while comparison on the basis of gadolinium would fail due to the absence of Gd-DTPA-DSA lipid on bare silica particles. Similarly to the fluorescence experiments, it was observed that lipid-coated silica particles accumulated gradually in the liver, while negligible amounts of cadmium, and thus contrast agent, were found in the kidneys, lungs, and heart (Figure 6, panels A and B). Different from the fluorescence imaging results, the ICP-MS results now also revealed a gradual uptake of lipid-coated particles in the spleen. This discrepancy between the results obtained through fluorescence imaging and ICP-MS was also observed for the bare silica particles and was attributed to the high absorbance of the QD emission by the spleen (which clears and thus contains a high amount of redundant red blood cells). In comparison to the lipid-coated particles, ICP-MS indicated that bare silica particles accumulated within 1 h in liver and spleen and to a higher extent than that observed for the lipid-coated nanoparticles, emphasizing their poor pharmacokinetics and possibly their higher exposure to opsonins (Figure 6, panels C and D). In addition, these particles were also observed to accumulate in the lungs, to cause breathing problems and to cause liver necrosis (Figure 1 in Supporting Information). Three (out of 11) mice died after bare silica particles were administered, while no acute adverse effects were observed after the administration of

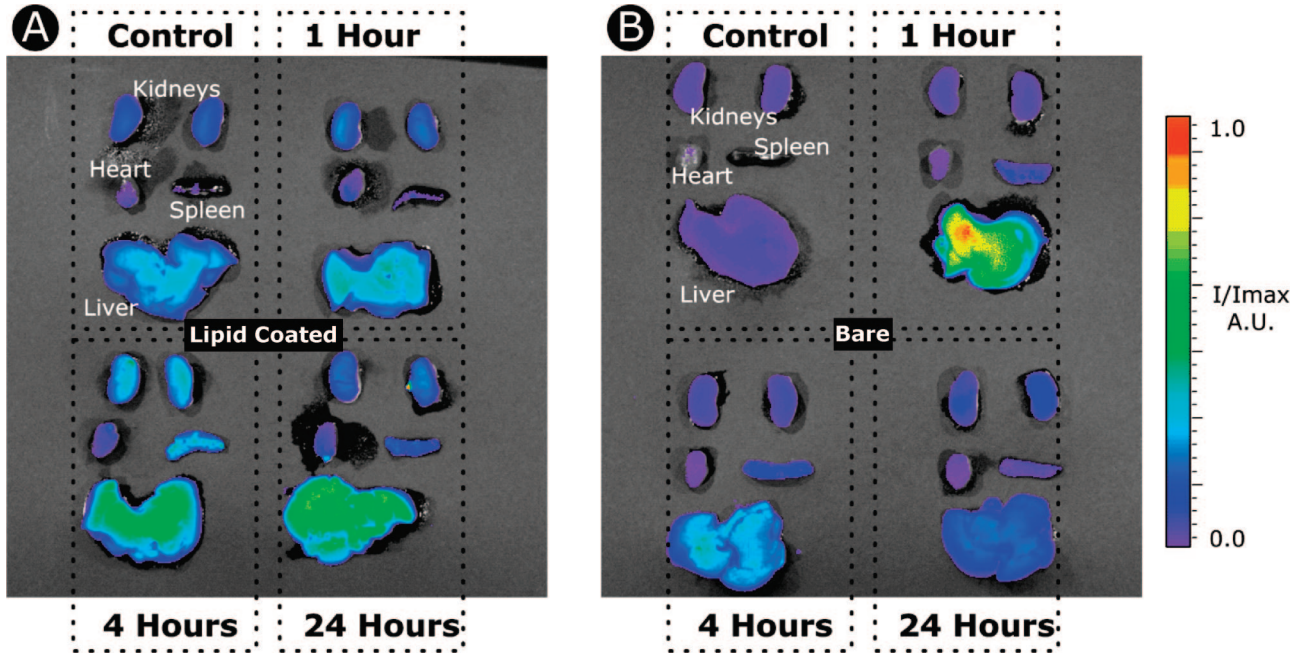

Figure 5. Fluorescence imaging of liver, spleen, kidneys, and heart of control mice and mice sacrificed 1, 4, and 24 h postinjection with (A) Q-SiPaLCs and (B) Q-Sis. While an immediate uptake of bare silica particles in the liver was observed, the lipid-coated silica particles accumulated gradually over time in the liver which is in agreement with their prolonged circulation half-life value ($n = 2$).

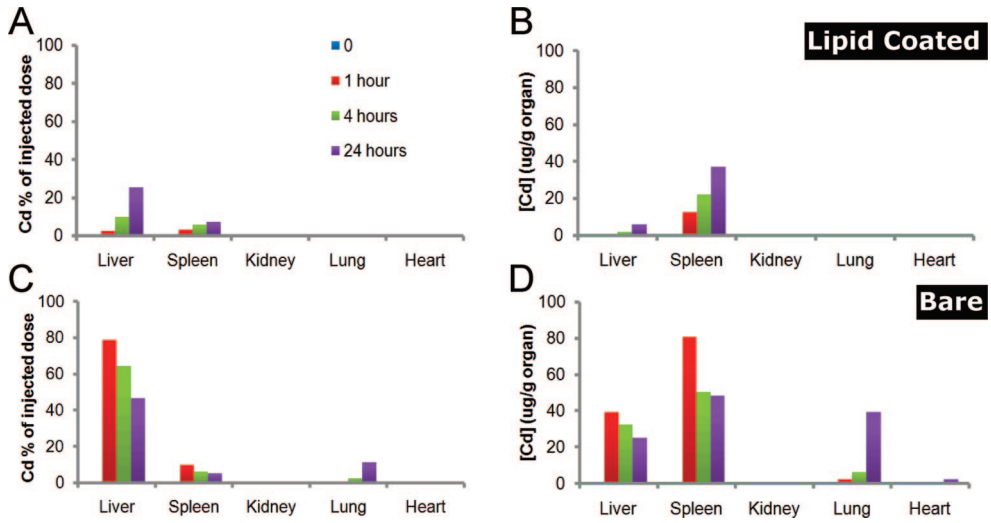

Figure 6. ICP-MS cadmium quantification in liver, spleen, kidneys, lungs, and heart of control mice and mice sacrificed 1, 4, and 24 h postinjection with (A, B) Q-SiPaLCs and (C, D) Q-Sis ($n = 1$). The values are both given as percentage of injected dose (A and C) and as a cadmium, and thus particle, density in organs (B and D). The lipid coating of silica particles prevents particle accumulation in lungs.

lipid-coated silica particles. Mice injected with lipid-coated silica particles did not show particle accumulation in the lungs and did not suffer from breathing problems or liver necrosis, which demonstrates the effectiveness of the lipid coating in improving silica particle bioapplicability. It must further be noted that only ~1/3 of the lipid-coated and ~2/3 of the bare particles were retrieved 24 h postinjection in the analyzed organs. Considering the half-life values (~165 and ~15 min, respectively) it is unlikely that the remaining particles were still present in the blood. Previous studies with bare silica particles reported small amounts of the particles (typically <10%) to be present in muscles and bone marrow and 20−40% of the particles in the gastrointestinal tract, urine, and feces (after 24 h), indicative of particle clearance.[6,37] It remains unclear whether the relatively low recovery for the lipid-coated particles is due to distribution into other (not analyzed) organs or that the lipid-coating facilitates the silica particle clearance after uptake in organs.

The distribution of the nanoparticles at the cellular level was investigated by CSLM (Figure 7). Mice were sacrificed 24 h postinjection of Q-SiPaLCs and Q-Sis and organ sections were taken from the liver, spleen, kidneys, lungs, and heart. The sections were stained for cell nuclei using DAPI (blue), for macrophages using Rat-Anti-Mouse CD68-Alexa-647 (green), and for endothelial cells by intravenous injection of isolectin-Alexa-488 (green) 15 min before

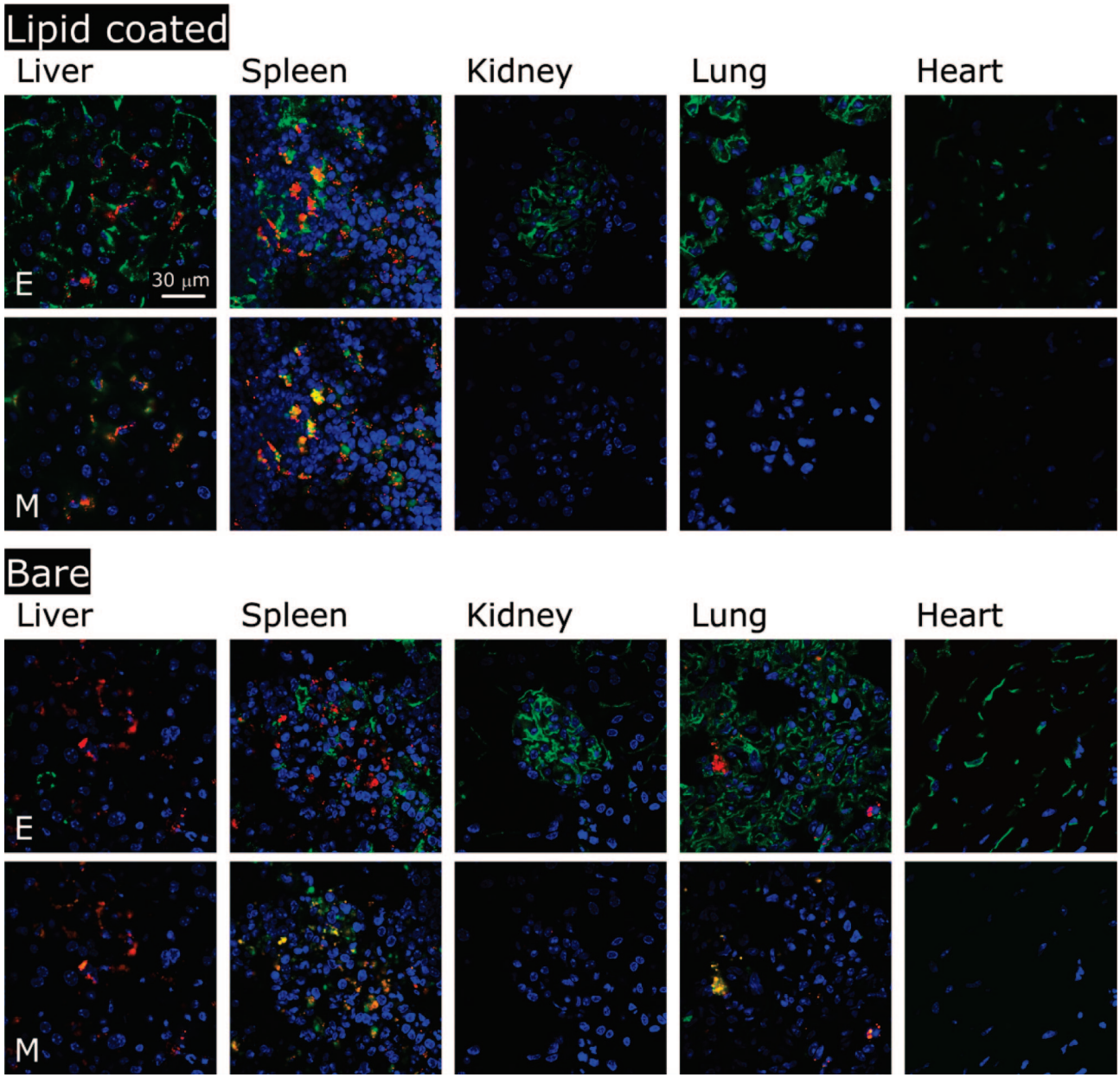

Figure 7. CLSM of mice organs sacrificed 24 h postinjection with lipid-coated (Q-SiPaLCs) or bare (Q-Sis) silica particles. Cell nuclei (blue), QDs (red), and endothelium or macrophages (both in green, but in separate panels indicated with E and M, respectively) were visualized and revealed colocalization of both particles with macrophages. The scale bare in the upper left panel applies to all panels.

sacrifice.[56] Red fluorescence signal originated from the QDs for both the lipid-coated and the bare silica particles. Three fluorescence signals were imaged simultaneously each time, in the course of which the red QD signal and the blue DAPI signal were held constant, but the third signal was recorded with filter sets suited for either endothelial cell or macrophage related fluorescence. Both signals are shown in green in separate sets of CSLM images of organ sections in Figure 7. The lipid-coated silica particles were clearly visible in liver and spleen (Figure 7A). In addition, the lectin stain for endothelium cells marked the vasculature, which was best recognized in the vascular knots observed in the kidneys, indicating glomeruli (capillary tufts specific to kidneys). The macrophage stain further revealed a high degree of colocalization between the nanoparticles and macrophages (or Kupffer cells, the name for macrophages in the liver). Endocytosis of the lipid-coated silica particles, which contained PEGylated lipids, was expected, since a wide range of long-circulating PEGylated particles are eventually taken up by macrophages.[38] Bare silica particles not only were present in liver and spleen but also were observed in the lungs and were established to be widely taken up by macrophages in all of these three organs (Figure 7B).

Besides imaging on a macroscopic (entire organs) and microscopic scale (organ tissue sections), the organs were investigated at the nanometer or subcellular level using energy dispersion spectroscopy (EDS) and TEM (Figure 8). Sections of the organs, from mice sacrificed 24 h postinjection, were fixed in glutaraldehyde and stained with electron-dense osmium tetroxide, uranyl acetate, and Reynold's lead

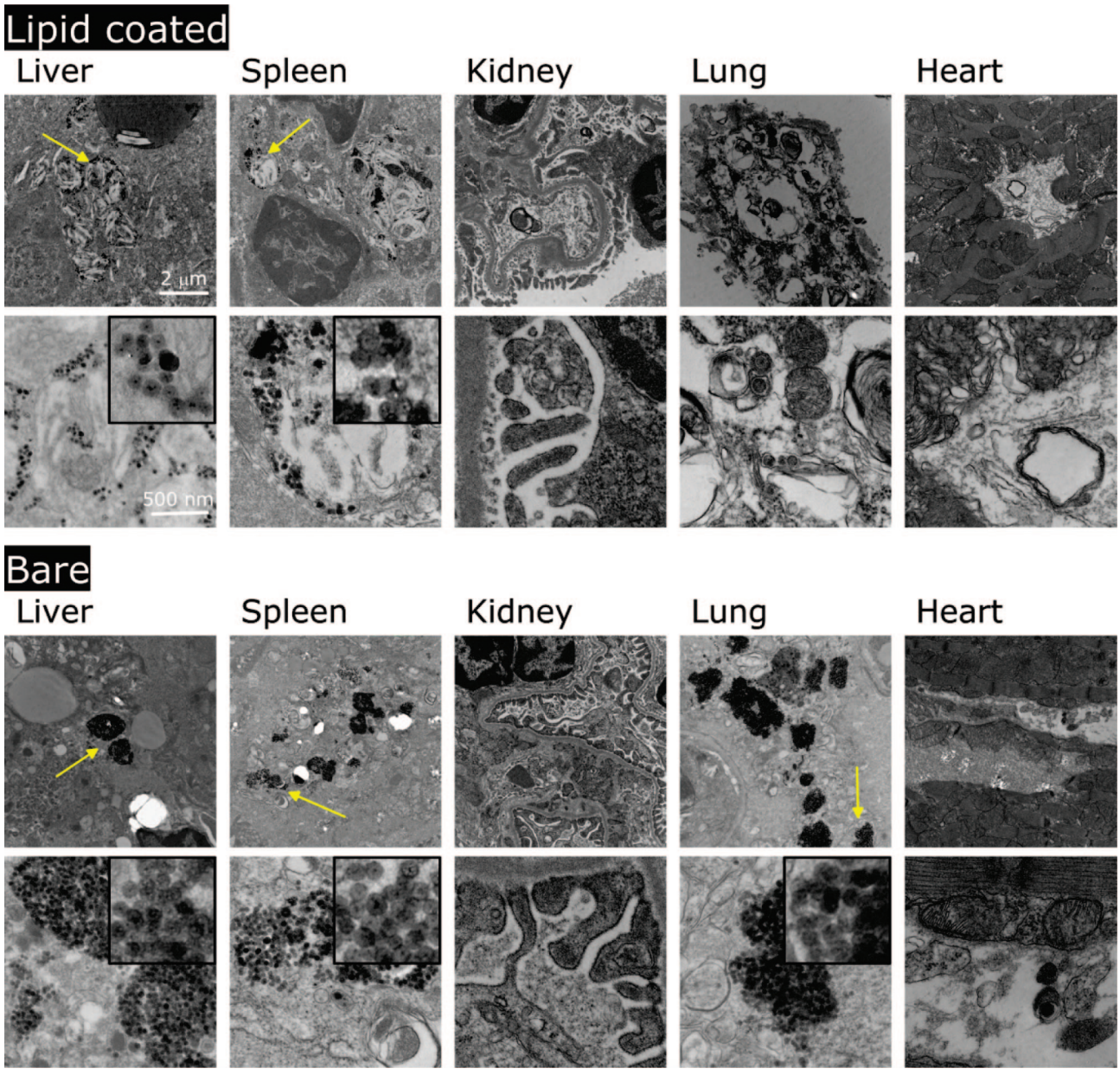

Figure 8. TEM images of mice organs sacrificed 24 h postinjection with Q-SiPaLCs or Q-Sis. The 2 μm scale bar in the upper left panel applies to all upper row panels (for lipid-coated and bare), while the 500 nm scale bar applies to all lower row panels (lipid-coated and bare). The lower row panels are magnifications of the regions indicated by yellow arrows in the upper row panels. In the insets single silica particles with the dense QD core can be clearly identified.

citrate. EDS experiments proved the presence of silica particles (Figure 2 in Supporting Information). The TEM experiments not only allowed single silica particle tracking in organs but also revealed important information about the state of the nanoparticles and their subcellular localization. First of all, lipid-coated silica particles were observed to be present in macrophages in liver and spleen and to a small extent in liver hepatocytes. More specifically, the particles were observed to be localized in lysosomal parts of macrophage cells. Thirdly, and of vital importance, we observed that lipid-coated silica particles remained rather well-dispersed in the organs, whereas bare silica particles were aggregated to a much larger extent (see the lower row panels for mice injected with bare silica particles). The bare silica particle aggregates were mostly found in or adjacent to vasculature. In the lungs, aggregates were found to block the capillaries. This confirmed that charge stabilized silica suspensions are prone to aggregation under physiological conditions and that they are filtered from the blood in the first capillary bed encountered: the mouse lungs following tail vein injection.[38] The accumulation of bare silica particles in mouse and rat lungs after tail vein injection has been observed previously and was attributed to particle aggregation.[6,24,37] Finally, we note that the amount of particle aggregation probably plays a crucial role in the way particles are cleared from organs and the body. Although not studied here, it is possible that well-dispersed particles are better excreted from the body.

In conclusion, we have studied the short-term cytotoxicity (3 days in vitro and 1 day in vivo) and the pharmacokinetics

of lipid-coated and bare silica nanoparticles. These bioapplicable particles were prepared using a general and versatile method that we recently developed. The results showed that the PEG-lipid coating increased the blood circulation half-life time of silica particles by a factor of 10 (165 min vs 15 min for lipid-coated or bare silica particles, respectively). This relatively long circulation half-life time as compared to earlier reported values in the order of a few minutes, suffices for most targeting applications of silica-based diagnostics and therapeutics. Furthermore, the lipid coating of silica particles results in a favorable tissue distribution profile as compared to the bare silica particles, as shown at organ level (MRI, FI, and ICP-MS), at tissue level (CSLM) and at cellular or nanoparticle level (TEM). The lipid coating proved effective in preventing silica particles from aggregation, and thereby preventing clogging of capillaries in the lung and liver. Despite the observed and multiple short-term advances of lipid-coated over bare particles, it must be stressed however that the long-term effects or the effects of multiple doses were not investigated in the present study. Nevertheless, this work shows that coating of silica-based nanoparticles with PEG-lipids is an important step toward solving the issue of the bioapplicability of silica particles and makes them promising candidates for drug delivery, gene therapy, and molecular imaging.

Acknowledgment. Confocal laser scanning microscopy was performed at the MSSM-Microscopy Shared Resource Facility, supported with funding from NIH-NCI shared resources grant (5R24 CA095823-04), NSF Major Research Instrumentation grant (DBI-9724504) and NIH shared instrumentation grant (1 S10 RR0 9145-01). Fluorescence imaging was performed in the MSSM In Vivo Imaging Shared Research Facility. Partial support was provided by NIH/NHLBI R01 HL71021 and NIH/NHLBI R01 HL78667 (Z.A.F.).

Supporting Information Available: Synthesis procedures of the nanoparticles, experimental details, and supporting figures showing signs of liver necrosis for mice injected with bare silica particles and EDS on silica particles in the liver. This material is available free of charge via the Internet at http://pubs.acs.org.

References

(1) Stober, W.; Fink, A.; Bohn, E. *J. Colloid Interface Sci.* **1968**, *26* (1), 62–&.
(2) Osseoasare, K.; Arriagada, F. J. *Colloids Surf.* **1990**, *50*, 321–339.
(3) O. D. Velev, E. W. K. *Adv.Mater.* **2000**, *12* (7), 531–534.
(4) Vallet-Regí, M.; Balas, F.; Arcos, D. *Angew. Chem., Int. Ed.* **2007**, *46* (40), 7548–7558.
(5) Lu, J.; Liong, M.; Zink, J. I.; Tamanoi, F. *Small* **2007**, *3* (8), 1341–1346.
(6) Barbé, C.; Bartlett, J.; Kong, L.; Finnie, K.; Lin, H. Q.; Larkin, M.; Calleja, S.; Bush, A.; Calleja, G. *Adv. Mater.* **2004**, *16* (21), 1959–1966.
(7) Trewyn, B. G.; Giri, S.; Slowing, I. I.; Lin, V. S.-Y. *Chem. Commun.* **2007**, 3236–3245.
(8) Maver, U.; Godec, A.; Bele, M.; Planinsek, O.; Gaberscek, M.; Srcic, S.; Jamnik, J. *Int. J. Pharm.* **2007**, *330*, 164–174.
(9) Doadrio, J. C.; Sousa, E. M. B.; Izquierdo-Barba, I.; Doadrio, A. L.; Perez-Pariente, J.; Vallet-Regi, M. *J. Mater. Chem.* **2006**, *16*, 462–466.
(10) Chowdhury, E. H.; Akaike, T. *Curr. Gene Ther.* **2005**, *5* (6), 669–676.
(11) Kneuer, C.; Sameti, M.; Haltner, E. G.; Schiestel, T.; Schirra, H.; Schmidt, H.; Lehr, C.-M. *Int. J. Pharm.* **2000**, *196* (2), 257–261.
(12) Roy, I.; Ohulchanskyy, T. Y.; Bharali, D. J.; Pudavar, H. E.; Mistretta, R. A.; Kaur, N.; Prasad, P. N. *Proc. Natl. Acad. Sci.U.S.A.* **2005**, *102* (2), 279–284.
(13) Slowing, I. I.; Trewyn, B. G.; Lin, V. S. Y. *J. Am. Chem. Soc.* **2007**, *129* (28), 8845–8849.
(14) Chen, F. Q.; Gerion, D. *Nano Lett.* **2004**, *4* (10), 1827–1832.
(15) Selvan, S. T.; Tan, T. T.; Ying, J. Y. *Adv. Mater.* **2005**, *17* (13), 1620.
(16) Praetorius, M.; Brunner, C.; Lehnert, B.; Klingmann, C.; Schmidt, H.; Staecker, H.; Schick, B. *Acta Oto-Laryngol.* **2007**, *127* (5), 486–490.
(17) Gerion, D.; Herberg, J.; Bok, R.; Gjersing, E.; Ramon, E.; Maxwell, R.; Kurhanewicz, J.; Budinger, T. F.; Gray, J. W.; Shuman, M. A.; Chen, F. F. *J. Phys. Chem. C* **2007**, *111* (34), 12542–12551.
(18) Taylor, K. M. L.; Kim, J. S.; Rieter, W. J.; An, H.; Lin, W.; Lin, W. *J. Am. Chem. Soc.* **2008**, *130* (7), 2154–2155.
(19) Rieter, W. J.; Kim, J. S.; Taylor, K. M. L.; An, H.; Lin, W.; Tarrant, T.; Lin, W. *Angew. Chem., Int. Ed.* **2007**, *46* (20), 3680–3682.
(20) Bakalova, R.; Zhelev, Z.; Aoki, I.; Ohba, H.; Imai, Y.; Kanno, I. *Anal. Chem.* **2006**, *78* (16), 5925–5932.
(21) Selvan, S. T.; Patra, P. K.; Ang, C. Y.; Ying, J. Y. *Angew. Chem., Int. Ed.* **2007**, *46* (14), 2448–2452.
(22) Lee, J. H.; Jun, Y. W.; Yeon, S. I.; Shin, J. S.; Cheon, J. *Angew. Chem., Int. Ed.* **2006**, *45* (48), 8160–8162.
(23) Yoon, T. J.; Yu, K. N.; Kim, E.; Kim, J. S.; Kim, B. G.; Yun, S. H.; Sohn, B. H.; Cho, M. H.; Lee, J. K.; Park, S. B. *Small* **2006**, *2* (2), 209–215.
(24) Bridot, J.-L.; Faure, A.-C.; Laurent, S.; Riviere, C.; Billotey, C.; Hiba, B.; Janier, M.; Josserand, V.; Coll, J.-L.; VanderElst, L.; Muller, R.; Roux, S.; Perriat, P.; Tillement, O. *J. Am. Chem. Soc.* **2007**, *129* (16), 5076–5084.
(25) Lu, C. W.; Hung, Y.; Hsiao, J. K.; Yao, M.; Chung, T. H.; Lin, Y. S.; Wu, S. H.; Hsu, S. C.; Liu, H. M.; Mou, C. Y.; Yang, C. S.; Huang, D. M.; Chen, Y. C. *Nano Lett.* **2007**, *7* (1), 149–154.
(26) Sharma, P.; Brown, S.; Walter, G.; Santra, S.; Moudgil, B. *Adv. Colloid Interface Sci.* **2006**, *123−126*, 471–485.
(27) Yi, D. K.; Selvan, S. T.; Lee, S. S.; Papaefthymiou, G. C.; Kundaliya, D.; Ying, J. Y. *J. Am. Chem. Soc.* **2005**, *127* (14), 4990–4991.
(28) Yang, H. S.; Santra, S.; Walter, G. A.; Holloway, P. H. *Adv. Mater.* **2006**, *18* (21), 2890.
(29) Salgueiriño-Maceira, V.; Correa-Duarte, M. A.; Spasova, M.; Liz-Marzán, L. M.; Farle, M. *Adv. Funct. Mater.* **2006**, *16* (4), 509–514.
(30) Liu, N. G.; Prall, B. S.; Klimov, V. I. *J. Am. Chem. Soc.* **2006**, *128* (48), 15362–15363.
(31) Park, K.; Liang, G.; Ji, X.; Luo, Z. P.; Li, C.; Croft, M. C.; Markert, J. T. *J. Phys. Chem. C* **2007**, *111* (50), 18512–18519.
(32) Santra, S.; Yang, H. S.; Holloway, P. H.; Stanley, J. T.; Mericle, R. A. *J. Am. Chem. Soc.* **2005**, *127* (6), 1656–1657.
(33) Liang, S.; Wang, Y.; Zhang, C.; Liu, X.; Liu, Z.; Xu, R.; Yin, D. *J. Radioanal. Nucl. Chem.* **2006**, *269* (1), 3–7.
(34) Lai, C. W.; Wang, Y. H.; Lai, C. H.; Yang, M. J.; Chen, C. Y.; Chou, P. T.; Chan, C. S.; Chi, Y.; Chen, Y. C.; Hsiao, J. K. *Small* **2008**, *4* (2), 218–224.
(35) Levy, L.; Sahoo, Y.; Kim, K. S.; Bergey, E. J.; Prasad, P. N. *Chem. Mater.* **2002**, *14* (9), 3715–3721.
(36) Roy, I.; Ohulchanskyy, T. Y.; Pudavar, H. E.; Bergey, E. J.; Oseroff, A. R.; Morgan, J.; Dougherty, T. J.; Prasad, P. N. *J. Am. Chem. Soc.* **2003**, *125* (26), 7860–7865.
(37) Borchardt, G.; Brandriss, S.; Kreuter, J.; Margel, S. *J. Drug Targeting* **1994**, *2* (1), 61–77.
(38) Moghimi, S. M.; Hunter, A. C.; Murray, J. C. *Pharmacol. Rev.* **2001**, *53* (2), 283–318.
(39) Gref, R.; Domb, A.; Quellec, P.; Blunk, T.; Muller, R. H.; Verbavatz, J. M.; Langer, R. *Adv. Drug Delivery Rev.* **1995**, *16*, 215–233.
(40) Vanblaaderen, A.; Vrij, A. *J. Colloid Interface Sci.* **1993**, *156* (1), 1–18.
(41) Kim, J.; Lee, J. E.; Lee, J.; Jang, Y.; Kim, S. W.; An, K.; Yu, J. H.; Hyeon, T. *Angew. Chem., Int. Ed.* **2006**, *45* (29), 4789–4793.
(42) Kumar, R.; Roy, I.; Ohulchanskyy, T. Y.; Goswami, L. N.; Bonoiu, A. C.; Bergey, E. J.; Tramposch, K. M.; Maitra, A.; Prasad, P. N. *ACS Nano* **2008**, *2*, 449–456.
(43) Bagwe, R. P.; Hilliard, L. R.; Tan, W. *Langmuir* **2006**, *22* (9), 4357–4362.
(44) Huo, Q.; Liu, J.; Wang, L. Q.; Jiang, Y.; Lambert, T. N.; Fang, E. *J. Am. Chem. Soc.* **2006**, *128* (19), 6447–6453.
(45) Jo, S.; Park, K. *Biomaterials* **2000**, *21* (6), 605–616.

(46) Xu, H.; Yan, F.; Monson, E. E.; Kopelman, R. *J. Biomed. Mater. Res., Part A* **2003**, *66*, 870–879.
(47) Alcantar, N. A.; Aydil, E. S.; Israelachvili, J. N. *J. Biomed. Mater. Res.* **2000**, *51*, 343–351.
(48) Yang, C. Y.; Cai, S. J.; Liu, H.; Pidgeon, C. *Adv. Drug Delivery Rev.* **1997**, *23* (1−3), 229–256.
(49) Troutier, A.-L.; Ladaviere, C. *Adv. Colloid Interface Sci.* **2007**, *133* (1), 1–21.
(50) Mornet, S.; Lambert, O.; Duguet, E.; Brisson, A. *Nano Lett.* **2005**, *5* (2), 281–285.
(51) Linseisen, F. M.; Hetzer, M.; Brumm, T.; Bayerl, T. M. *Biophys. J.* **1997**, *72*, 1659–1667.
(52) Koole, R.; Van Schooneveld, M. M.; Hilhorst, J.; Castermans, K.; Cormode, D. P.; Strijkers, G. J.; de Mello Donega, C.; Vanmaekelbergh, D.; Griffioen, A. W.; Nicolay, K.; Fayad, Z. A.; Meijerink, A.; Mulder, W. J. M. Submitted for publication.
(53) Xie, R. G.; Kolb, U.; Li, J. X.; Basche, T.; Mews, A. *J. Am. Chem. Soc.* **2005**, *127* (20), 7480–7488.
(54) Koole, R.; van Schooneveld, M. M.; Hilhorst, J.; de Mello, D.; Celso, n/a; Hart, D. C.; van Blaaderen, A.; Vanmaekelbergh, D.; Meijerink, A. *Chem. Mater.* **2008**, *20* (7), 2503–2512.
(55) Marque, V.; Kieffer, P.; Gayraud, B.; Lartaud-Idjouadiene, I.; Ramirez, F.; Atkinson, J. *Arterioscler., Thromb., Vasc. Biol.* **2001**, *21* (7), 1184–1189.
(56) Dickie, R.; Bachoo, R. M.; Rupnick, M. A.; Dallabrida, S. M.; DeLoid, G. M.; Lai, J.; DePinho, R. A.; Rogers, R. A. *Microvasc. Res.* **2006**, *72* (1−2), 20–26.

NL801596A